Aust. Met. Mag. 39 (1991) 1–9

Predictability studies of the Antarctic atmosphere

Klaus Fraedrich* **and Lance Leslie**
Bureau of Meteorology Research Centre, Melbourne, Australia
(Manuscript received April 1990; revised August 1990)

In this study estimates are made of the predictability time-scales for the Weddell Sea section of the Antarctic region. Two distinct methods were applied.
One of the methods used was a traditional approach due to Lorenz in which the rate of separation of initially close atmospheric states (analogues) was calculated. It was found here that even the best 500 hPa height field analogues were only mediocre and that root mean square differences between the analogues grew very rapidly, suggesting that the predictability time-scales might be quite short. However, the absence of very good analogues shows that an analogue approach is probably not suitable for the Weddell Sea region, and the predictability estimates obtained should be treated with caution.
An alternative approach, in which recently developed chaos theory, also known as non-linear systems analysis, was applied to the Australian Bureau of Meteorology archived analyses of 500 hPa cyclone track positions, was also investigated. The divergence of initially close pieces of cyclone tracks was derived from the algorithm of Grassberger and Procaccia (1984). The results suggest the existence of a low-dimensional attractor, describing the dynamics of the weather systems, of fractal dimension somewhere between 5 and 6. Rates of separation calculated from this algorithm also gave short predictability time-scale estimates of about one day for the error doubling time. These results are consistent with estimates of error doubling times found by studies of other baroclinically active regions of the globe.

Introduction

There is a growing interest in the application of numerical weather prediction (NWP) systems to the Antarctic region, as the increasing scientific and economic importance of the region is being recognised. The Australian Bureau of Meteorology, in particular, is currently developing a regional Antarctic NWP data assimilation system for short-term, high-resolution (approximately 90 km) operational prediction out to 48 hours. As part of the development of forecasting strategies for the region, estimates of predictability time-scales for Antarctica are very important as they will give an indication of the time-scales for which the deterministic NWP forecasts will be valid.

The predictability of a dynamical system like the atmosphere is closely related to the problem of its stability during its time evolution, and a relevant measure of the potential predictability of a dynamical system is the rate at which initially small errors grow. Early studies of the potential predictability of meteorological systems were based on the analogue approach described by Lorenz (1969), and two basic measures were introduced for quantification: the doubling (or e-folding) time of initially small errors, and a time-scale after which initially close weather patterns have lost their similarity. In recent years, however, new techniques have been developed for measuring the predictability of dynamical systems. These are the so-called non-linear systems analysis techniques (see, for example, Eckmann and Ruelle (1985); Lorenz (1985)) which form part of the rapidly developing theory of chaos.

There are two basic properties characterising the atmosphere as a non-linear dynamical system: the dimension and the entropy. Dimension is a static measure of a dynamical system describing the degrees of freedom involved; if the dimension

Corresponding author address: Dr Lance Leslie, Bureau of Meteorology Research Centre, GPO Box 1289K, Melbourne 3001, Australia.
*On leave from the Institute for Meteorology, Free University of Berlin.

is fractal, it indicates chaotic behaviour which, in a qualitative sense, is related to a sensitive dependence on initial conditions. Initially close weather states do not remain as nearest neighbours but spread with increasing time; though similar, they are distinct (because of the fractal structure of the attractor). The entropy is a measure of the degree of chaos and characterises this spread of initially close trajectories in phase space. In this sense the entropy measures the predictability of a system in terms of a rate of divergence of initially close weather patterns. If estimated from data it describes a natural (or potential) predictability of the system as will be discussed in this study.

In a study of the predictability of tropical cyclone tracks in the Australian region, Fraedrich and Leslie (1989) applied non-linear systems analysis techniques to tropical cyclone storm tracks. The divergence of initially close pieces of tropical cyclone tracks was calculated by suitably averaging their rate of separation, using the algorithm of Grassberger and Procaccia (1984). The method described by Fraedrich and Leslie can be used for other meteorological systems in different parts of the globe and in the investigation described below it is used to provide predictability estimates for 500 hPa cyclone storm track data in the Weddell Sea sector of Antarctica. These estimates are compared with those obtained from the older, analogue approach to predictability. It is noted that the Australian Bureau of Meteorology archived operational data used in the present study are composed to a considerable extent of satellite retrievals and interpreted satellite imagery. While these data are of lower quality than conventional data, they are now available twice daily on the Global Telecommunication System (GTS) and are used operationally by the major global numerical weather prediction centres, such as the European Centre for Medium Range Weather Forecasts (ECMWF) (Shaw et al. 1987).

Finally, two points should be emphasised. First, that the non-linear systems analysis as described in this study focuses largely on the predictability time-scales of a particular system, in this case the high-latitude cyclones of the Weddell Sea region, using observational data. In that sense it differs from the analogue approach and also from the recent work on the predictability characteristics of numerical models, which cover a whole range of weather phenomena resolvable by the model, thereby including other systems (for example, anticyclones as well as cyclones) which could have quite different predictability time-scales. Second, that although this study is concerned with predictability estimates based on observations, it should be pointed out that a large and growing body of work on the predictive ability of NWP models also exists (see, for example, the recent extensive survey by Murphy (1990)). Inadequacies in both initial conditions and model formulation (Smagorinsky 1969; Miyakoda et al. 1972) determine the predictability of a NWP model.

Methodology and data

The traditional approach (using analogues)
This method calculates the distance between two only slightly different initial atmospheric states evolving in time. In an atmospheric model one solves the non-linear equations twice with different sets of initial conditions (Thompson 1957; Smagorinsky 1969):

$$\frac{dx_i}{dt} = f_i\,(x_i\,, \ldots, x_n) \qquad \ldots 1$$

with n suitably normalised variables x_i. Denoting an initial weather state, or realisation, by a vector $\underset{\sim}{x} = (x_i\,, \ldots, x_n)$ in the n-dimensional phase space, and another realisation by a vector deviation $\underset{\sim}{x} + \delta\underset{\sim}{x}$, then their Euclidean distance

$$D(t) = (\delta\underset{\sim}{x}\,.\,\delta\underset{\sim}{x})^{1/2} \qquad \ldots 2$$

is proportional to the root mean square error (rms) of the deviation. The time limit of predictability can be determined by the time required for the Euclidean distance D(t) to evolve to a state in which it oscillates about a saturation value D_{sat}, not greater than that calculated from two randomly selected states of the system. If the distance is below this threshold, one would expect the predictability to be longer.

Actual atmospheric observations have been used in only a few predictability studies. Here the two initially close but different states $\underset{\sim}{x}$ and $\underset{\sim}{x} + \delta\underset{\sim}{x}$ are obtained from analogue pairs of past weather maps (Lorenz 1969; Gutzler and Shukla 1984). Pairs of observed analogues have generally been found to be only of mediocre quality. They yield doubling times of 6–8 days for hemispheric and 3–4 days for regional scales; that is, larger errors grow less rapidly than initially small errors because they approach a saturation level. Therefore, approximate theories for error growth have been developed (Lorenz 1969, 1985; Kalnay and Livezey 1985) from which the growth of small errors can be inferred.

Logistic error growth. Randomly chosen small errors are represented in the phase space of the dynamical system by an infinitesimally small sphere which eventually expands into an error ellipsoid. Assuming the semi-axis with the largest expansion rate, λ_1, to contribute most to the overall error growth, the magnitude of the error will then be governed approximately by the equation

$$\frac{dD}{dt} = \lambda_1 D\,. \qquad \ldots 3$$

The common measure of the error growth, its doubling time T, is then given by $T = \ln 2/\lambda_1$.

Errors, however, do not undergo Malthusian growth but reach a saturation level, D_{sat}, which is due to the non-linearity of the system. Lorenz (1969) included this by a quadratic limitation of the growth rate to obtain the Verhulst equation with the familiar logistic solution

$$\frac{dD}{dt} = \lambda_1 D - cD^2, \qquad ...4$$

which has the limiting value $D_{sat} = \lambda_1/c$. Although there is no rigorous justification for Eqn 4 it seems to be plausible because, as Lorenz says, 'the principal nonlinear terms (which limit the error growth) in the atmospheric equations are quadratic and thus the nonlinear terms in the equations governing the field of errors will also be quadratic'. As a further extension, error growth should not be confined to the mode with the largest growth rate, λ_i, and all expanding semi-axes of the error sphere ($\lambda_i > 0$) with their related errors, D_i, need to be considered (Lorenz 1985).

Analogue data. The data consist of daily 0000 UTC southern hemisphere 500 hPa geopotential heights for a 15-year period (1972–1986). The data were derived from the archived Australian Bureau of Meteorology operational analyses on a polar stereographic projection with a resolution of about 380 km at 60°S. Linear interpolation in time was used to replace a few missing data. In this study we considered 500 hPa heights for the southern hemisphere winter months June, July and August in the Weddell Sea area, defined to be the region from 50° to 80°S and 80°W to 40°E. The annual cycle was removed from each grid-point by a parabolic best fit to the entire 15 winter time-series to provide 500 hPa height anomalies for further analysis.

Definition of analogues. The 500 hPa height anomalies are scaled by the cosine of latitude to obtain area-weighted daily weather maps $A_j(t)$ for $j = 1, \ldots, N$ grid-points. A measure of analogue quality is the rms difference between pairs of maps A_j, B_j. It is proportional to their Euclidean distance and is small for good analogues:

$$\text{rms}\,(t_A, t_B) = \frac{1}{N}\sum_{j=1}^{N}(A_j - B_j)^2. \qquad ...5$$

However, instead of minimising the distance between pairs of instantaneous daily maps (Lorenz 1969; Gutzler and Shukla 1984), analogues in the time evolution of weather patterns will be discussed. Thus, the distances between pairs of (at least) two-day sequences of daily weather maps are analysed, that is, rms (t_A, T_B) and rms ($t_A + 1$, $t_B + 1$).

The best analogues are found by comparing all 91 two-day sequences within a single winter with all two-day sequences of the remaining 14 winters. Thus we obtain a total number of 869 505 analogues. Only those from independent synoptic situations are chosen, to guarantee good analogues as recurrent circulation patterns and not generated by persistence.

An alternative approach (using non-linear systems analysis)

Storm track data. Storm tracks are constructed from 500 hPa lows by tracing their daily centres of minimum height during the fifteen Julys in the data period. However, whenever necessary, prior and subsequent days were added to document the life cycle of storms over the Weddell Sea as completely as possible. Only 26 of the total of 32 storm tracks analysed are shown in Fig. 1, to avoid clutter. They are shown in the two sets of 13 tracks labelled A–M (top) and N–Z (bottom). Qualitatively, the results show similarity with a ten-year climatology of cyclone tracks deduced from surface pressure maps (Kep 1984). The observed average duration of the 32 storm tracks (± standard deviation) is 6.4 ± 1.8 days. The mean initial position (± standard deviation) is 63.6° ± 7.1°S and 59.8° ± 12.5°W.

Distribution of distances between pairs of independent storms. Whereas the analogue method is used in a phase space defined by the weather map, a substitute phase space is constructed in applying the following non-linear systems analysis method. This phase space is spanned by delay-coordinates lagging a (scalar or vector) time-series of a dynamical system. Subsequently, a point in this substitute phase space, which embeds the dynamics of this system, corresponds to a piece of a time trajectory; its length is the number of lags used or, which is equivalent, is proportional to the embedding dimension of the substitute phase space. For sufficiently large embedding dimension, the substitute phase space retains the (attractor of the) dynamical system and its related static and dynamical properties, dimension and entropy, may be derived (Packard et al. 1980; Takens 1981): that is, the number of active modes involved in the process and the rate of divergence of initially close pieces of trajectories on the attractor. Applying this approach to storm tracks, their position vectors, $\underline{x}(t) = [x(t), y(t)]$, define the observed time-series and the sequence of lags provides the delay coordinate system of the substitute phase space, $\underline{x}_m(t_i) = [x(t_i), x(t_i + \tau), \ldots, x(t_i + (m-1)\tau)]$. Therefore, the number of all pairs of pieces of trajectories from independent storms, which are less than a distance l apart from one another (Grassberger and Procaccia 1983, 1984), can be deduced:

$$C_m(l) = \lim_{N\to\infty} N^{-2}\{\text{number of pairs } (t_i, t_j) \text{ with } r_{i,j} = \sum_{n=0}^{m-1}[x(t_i + n\tau) - x(t_j + n\tau)]^2 < l^2\}, \qquad ...6$$

where t_i and t_j belong to different (that is, independent) storm tracks. This number distribution function estimates an ensemble average over all independent pieces of storm trajectories (that is, positions in the phase space of time-lagged coordinates) which are less than the distance $r_{i,j} < l$ apart. Thus, $C_m(l)$ described the mean relative number of pairs of points which occurs in a phase space volume element (or ball) of radius l surrounding every individual piece of trajectory. With increasing distance threshold, l (or size of ball), the number of pairs of points grows. Furthermore, $C_m(l)$ changes its shape with increasing duration or length of the trajectory pieces (embedding dimension). Following Grassberger and Procaccia (1983), for a sufficiently large number N of points in phase space the distribution function, $C_m(l)$, leads to estimates of the dimension of attractors (D_2) and the divergence (K_2) of nearby pieces of trajectories evolving on them; that is, $C_m(l)$ scales for $m \to \infty$, $l \to 0$ as

$$C_m(l) \sim l^{D_2} \text{ EXP } (-m\,\tau\,K_2) \qquad ...7$$

Before actually estimating the cumulative distance distributions $C_m(l)$ for increasing embedding dimension m, the geographical distances between the individual pairs of independent storm positions need to be derived, that is, for relatively small distances

$$|x(t_i)-x(t_j)|^2 = R^2[\cos^2\{(\theta(t_i)+\theta(t_j))/2\} (\lambda(t_i) - \lambda(t_j))^2 + (\theta(t_i) - \theta(t_j))^2] \qquad ...8$$

which then enters the algorithm; $\theta(t)$, $\lambda(t)$ are the latitude and longitude of the storm positions, R is the earth's radius. Estimates of the cumulative distribution function are presented in a $\ln (C_m(l))$ versus $\ln l$ diagram for embedding dimensions $m = 1,2,3,\ldots$, that is, for pieces of trajectories lasting from one, two, three ..., etc. days.

The growth rates of errors in an atmospheric model (Lorenz 1965) can be determined by the set of i ($= 1,\ldots, n$) linear differential equations, whose coefficients $A(i, j) = \delta f_i/\delta x_j$ at x(t) are elements of the Jacobian matrix of Eqn 1 and vary with the time evolution (x(t), say). The eigenvectors of A(i, j) provide a local coordinate system which describes the semi-axes of an infinitesimally small error sphere expanding into an ellipsoid. After suitable time-averaging the associated positive characteristic exponents (that is, Lyapunov exponents), $\lambda_i(\underset{\sim}{x}_0, \delta\underset{\sim}{x}_0) > 0$, can be used to define predictability as the average rate of divergence of an infinitesimally small phase space volume, $K = \Sigma\lambda_i$, with $\lambda_i > 0$.

Applying this approach to atmospheric observations one should note that for smooth continuous evolution, this average growth rate, K, is equivalent to the average production of information per unit time (Kolmogoroff entropy). As the information production can also be defined in probabilistic terms, it can, at least in principle, be estimated from data. For practical purposes the order-2 entropy K_2 suffices as an estimator (see Grassberger and Procaccia (1983, 1984) and in particular Schuster (1988) for more details):

$$K \geqslant K_2 = -\lim \frac{1}{n\tau} \ln \sum_{i_0 \ldots i_n} p^2(i_0, \ldots, i_n), \qquad ...9$$

for $n \to \infty$, $\lambda \to 0$. The sum $\Sigma\, p^2(i_0, \ldots, i_n)$ is the probability that a pair of pieces of time trajectories in the state space (of dimension n) $\underset{\sim}{x}(t_i)$, $\underset{\sim}{x}(t_j)$, falls into the same sequence of boxes $(i_0, \ldots, i_{n-1})$ of the space-time (l, τ) partitioning with $(l, \tau) \to 0$, while the system evolves from (t_i, t_j) to $(t_i + n\tau, t_j + n\tau)$. This is equivalent to the probability that two independent pieces of trajectories of length or duration n remain less than a distance l apart. Estimates of the entropy are based on a counting algorithm of the relative number of sequences of trajectories in phase space, where $|\underset{\sim}{x}(t_i) - \underset{\sim}{x}(t_j)| < l, \ldots, |\underset{\sim}{x}(t_i + n\tau) - \underset{\sim}{x}(t_j + n\tau)| < l$, using a sufficiently large number of data points.

In this study the two methods described above are applied to study the predictability of the Antarctic atmosphere using observations. In the next section the results of the study are presented. The best past weather analogues and the time development of their ensemble mean rms errors are analysed. This is basically an error analysis in an Eulerian framework, which follows the more traditional approach. Storm tracks are also analysed and the related rate of divergence is estimated from nearby pieces of storm trajectories of independent tracks. This is basically a predictability analysis (on attractors) in the Lagrangian sense, which follows the alternative route.

Table 1. List of the ten best analogue pairs of 500 hPa geopotential height anomalies over the Weddell Sea region for the period 1972–1986, based on the rms height difference averaged over two consecutive days. The rms error shown in the Table is the minimum of the two consecutive daily differences, with the corresponding pairs of dates.

Analogue pairs	*Dates*	*rms error (m)*
1	8.7.76—17.6.82	26.1
2	17.7.85— 5.8.82	25.2
3	23.6.73—24.7.74	28.9
4	27.8.73—13.6.81	31.4
5	8.7.74— 8.6.84	30.0
6	23.7.72—16.7.84	29.1
7	17.7.79— 4.6.83	27.4
8	23.8.83—21.6.84	31.7
9	25.7.73—30.6.84	32.3
10	17.6.74—28.7.77	26.6

Fig. 1 **Climatology of July storm tracks over the Weddell Sea area deduced from daily 500 hPa height analyses (1972—1986).**

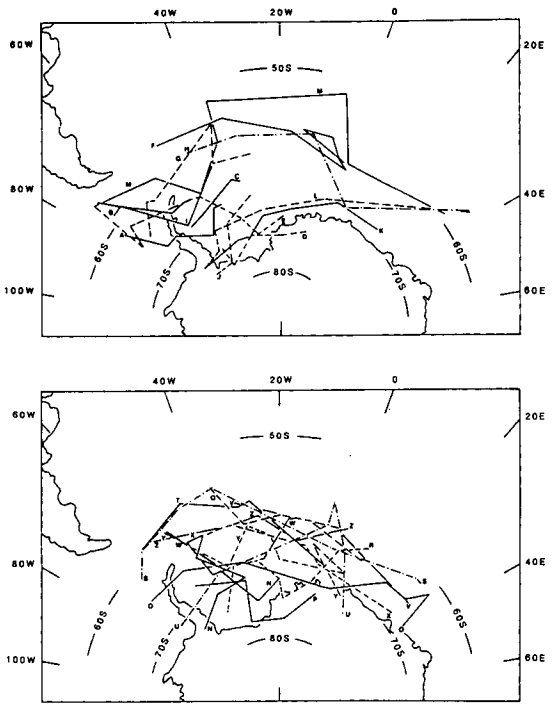

Results

Predictability estimates using past weather analogues

Analogue quality and error evolution. The ten best independent analogues and their related two-day sequential rms errors are listed in Table 1. Note that the dates refer to those pairs of days for which the one-day error rms (t_A, t_B) of the two-day sequence Eqn 8 is minimal. An example of an analogue pair of 500 hPa weather maps evolving in time is shown in the first two sets of three panels of Fig. 2. It is the second-best pair of analogues in terms of the two-day sequence of rms differences (and the fourth best if analogues are selected from one-day sequences). The daily rms evolutions of the analogues are composited about the minimum rms error. The ensemble means $<\text{rms}\ (t+m)>$ and the standard deviations are plotted in Fig. 3 for both positive and negative time lags, m. The following results should be noted:

(a) The symmetry between negative and positive time lags found by Lorenz (1969) is not obvious here. The error growth with progressing time ($m > 0$) appears to be initially more rapid than for time reversal. Also the standard deviation of errors is significantly different for the $m = 1$ and $m = -1$ time lags. The larger forward time error growth could possibly be an indication of sudden developments due to an instability in the flow, whereas the relatively slow approach towards similarity in the weather maps reflects a process less disturbed by instabilities.

Fig. 2 **An example of one of the best Weddell Sea weather analogues. Maps of the 500 hPa fields are shown for 18 July 1985 and 6 August 1986 with two consecutive days each. The 1986 analogue sequence is compared with 24 and 48-hour NWP model forecasts initialised on 6 August (see Fig. 6).**

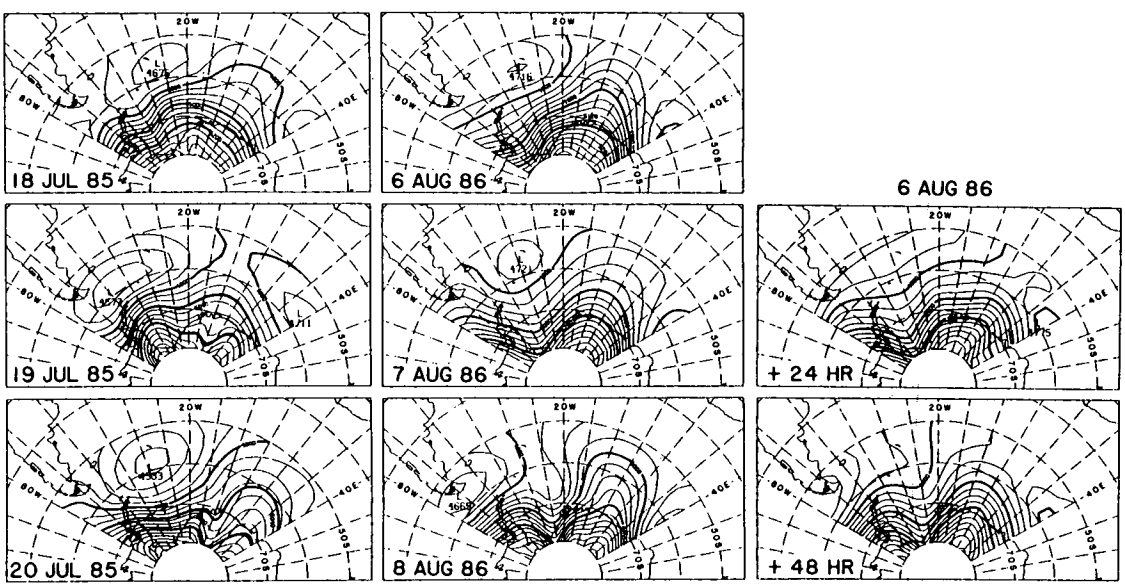

(b) After about m = 5 days the ensemble mean errors $<rms>$ of the analogue pairs rises to a saturation level $<rms_{sat}>$ of about 90 m.
(c) Compared with this saturation level the best analogues should not be judged as very good but rather, perhaps with the exception of m = 0, as mediocre for the study of the natural growth rate of small errors.
(d) Persistence forecasts are better than the best analogues, although their mean rms error, except for m = 1, lies within one standard deviation of the analogue ensemble average $<rms>$.

Estimating error growth. The estimates of error growth are based on the rms differences shown in Fig. 3. The growth rate can be determined after suitable normalisation by a saturation value

$$E(t) = \frac{<rms\ (t)>}{<rms_{sat}>} \qquad ...10$$

Fig. 3 Error evolution of daily best analogue pairs before and after error minimum. Averages and standard deviations are taken over the ten best analogues. The time-series is centred on the day of error minimum (lag 0). Persistence forecast errors are also shown for comparison.

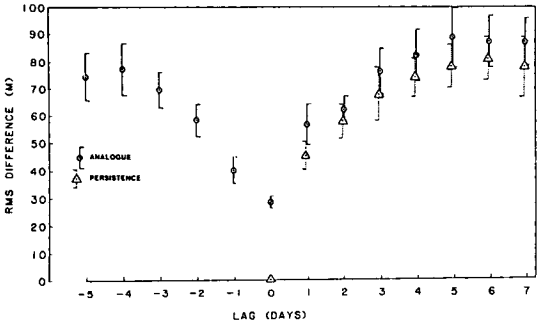

from an $E(t_0+1)$ versus $E(t_0)$ diagram (Fig. 4) using Eqns 3 and/or 4, where t_0 is any initial value. First, assuming errors to be initially small, that is, E = 0, doubling times are deduced from the slopes $dE(t_0+1)/dE(t_0) = \exp(+\lambda_1)$ through the origin (Fig. 4, upper margin). From the data points (t_0+1) one observes that only the first iteration, that is, E(0) to E(1), may be considered to be sufficient to provide a reasonable estimate of the error growth rate of initially small errors. This calculation gives a doubling time of T ~ 1 day. However, T increases to about 5–8 days for later time steps because the analogues have degraded rapidly and errors are approaching saturation (E ≒ 1). In this case, the quadratic (non-linear) effect is limiting the growth rates so that the solution of the logistic equation

Fig. 4 Observed values of errors, E, plotted in a E(t + 1) versus E(t) diagram. The errors are normalised by the ensemble mean saturation rms error $<rms_{sat}>$. The numbers in brackets refer to the time lags evolving from the day of error minimum (Fig. 2). Error doubling times are indicated on the upper and left margins as linear slopes through (E = 0) and (E = 1) for small and large errors (satisfying the model of logistic error growth).

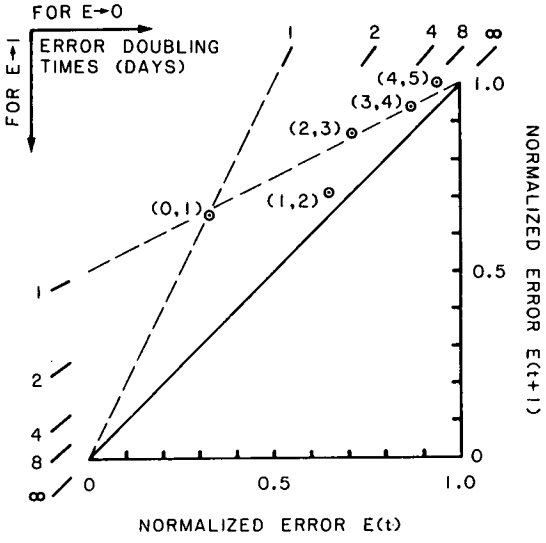

$$E(t_0+m) = E(t_0)/[\exp(-\lambda_1 m) + (1-\exp(-\lambda_1 m)\ E(t_0)] \qquad ...11$$

needs to be considered. Consequently, near saturation, predictability has to be estimated by the slope $dE(t_0+1)/dE(t_0) = \exp(-\lambda_1)$ of (1, 3) through E = 1 (left margin in Fig. 4). Now the error doubling time, $T = \ln 2/\lambda_1$, for initially small errors can be inferred from errors near saturation using the logistic equation (Eqns 3 or 4; see Lorenz (1969)). It appears that not only the first iteration (0, 1) with the largest growth rate but also all others (except the iteration (1, 2)) lie close to the same regression, leading to the error doubling time T ~ 1 day for initially small errors (as indicated on the left margin in Fig. 4). Furthermore, as the first iteration (0, 1) can be extrapolated to similar error growth rates using both E = 0 (Eqn 3) and E = 1 (Eqn 4), the best Antarctic analogues may be regarded as no better than mediocre (which was the same conclusion concerning analogue quality obtained by Lorenz (1969) or Gutzler and Shukla (1984) in their analogue studies). This, however, would increase the initial (0, 1) error growth rate to less than one day doubling time when the complete logistic solution is considered and not only near its boundaries (E = 0 or 1). Thus the initial growth rate estimate for E = 0 also satisfies the logistic equation.

Predictability estimates from non-linear systems analysis of storm track data. In this section, the chaos theory outlined above is now applied specifically to the tracks of 500 hPa cyclones in the Weddell Sea sector of Antarctica, as shown in Fig. 1.

Estimating predictability of storms (and their attractor dimension). The estimates of the attractor dimension are obtained from the slopes $C_m(l) \sim l^D$ of the ln $C_m(l)$ versus ln l graphs (Fig. 5, straight lines) for small l. These slopes tend to approach a saturation value of $D_2 \sim 5$–6 for embedding dimensions $m > 3$. The attractor is now embedded in a new phase space of delay coordinates. Its pointwise dimension, D_2, does not change if further coordinates are added to the embedding phase space. The dimension of the attractor provides a measure of the minimum number of independent variables necessary (but not sufficient) to model the dynamics of the system. This estimate coincides with similar results obtained from single-station surface pressure time-series (Fraedrich 1987) and 500 hPa heights (Essex et al. 1987), which provides further support for the hypothesis of low-dimensional attractor describing weather dynamics (see also Henderson and Wells (1988); Tsonis and Elsner (1988); Fraedrich and Leslie (1989)).

A non-integer (fractal) dimension characterises qualitatively the chaotic behaviour of a system (that is, its sensitive dependence on initial conditions) and thus provides evidence for the possible existence of a strange attractor governing the time evolution. The degree of chaos, however, is characterised by the Kolmogoroff entropy (or predictability), a lower bound of which is estimated by the order-2 entropy K_2 from Fig. 5 using Eqn 7. More specifically, the distance between the slopes, $C_m(l)$ and $C_{m+1}(l)$ for $m > 3$, (at a fixed small l) provides an estimate of the degree of chaos or (un)-predictability on attractors. Increasing the embedding dimension from m to m + 1 prolongs the pieces of trajectories by one time step. Thus the new cumulative distribution at fixed l describes the now reduced number of trajectory pairs which still remain within the distance $< l$, the others having exceeded it. Thus the change from C_m to C_{m+1} provides a measure of the mean separation rate (divergence) of two (initially close) pieces of trajectories. Their chance of diverging beyond the fixed threshold l during the next time step, τ, rises proportionally to exp $(+m\lambda_i\tau)$. On the other hand, their chances of remaining trapped within the threshold l decreases proportionally to the expansion rate along the principal axes of the growing error volume element, exp $(-m\lambda_i \tau)$; ie. $C_m \sim \exp(-m\tau(\lambda_1 + \lambda_2 + ..)) = \exp(-m\tau K_2)$, with $\tau_i > 0$. Therefore predictability is interpreted as an ensemble mean of the exponential expansion rate or divergence of (initially close $l \to 0$) pairs of pieces of trajectories; averaging occurs over all points on the attractor.

Fig. 5 Cumulative number distributions $C_m(l)$ of all pairs of storms which are less than a distance l apart. The first 26 of the storm tracks are shown in Fig. 4. The results are presented in a ln $C_m(l)$ versus ln l diagram; m denotes the number of consecutive storm days (that is, the embedding dimension) considered for the distance evaluation; l is the Euclidean distance.

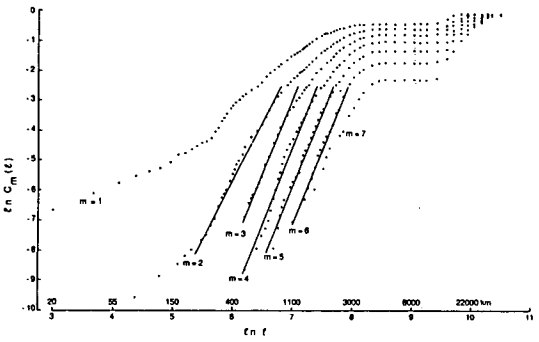

Thus, it is the difference between $\ln(C_m(l))$ and $\ln(C_{m+1}(l))$ at fixed l which yields a measure of the mean predictability from Eqn 7; that is, $K_2 = \ln(C_{m+1})/\tau$. The time-scale of predictability can be deduced from Fig. 5, $1/K_2 \sim 1$ day; this value reduced to about 0.7 days when considering doubling times of the rms errors. There is good agreement with one of the other non-linear analyses based on the 500 hPa heights (Essex et al. (1987), using Fig. 1), but not with the surface pressure analysis, where a time lag of the order of the autocorrelation time ($\tau = 3$ days, in comparison to $\tau = 1$ day) has been used to guarantee independent delay coordinates for the substitute phase space. Furthermore, it appears that very similar results are obtained applying the two different approaches to estimate predictability: (a) from the traditional approach of comparing past weather analogues occurring in an Eulerian frame; and (b) the non-linear systems analysis of the divergence of initially close pieces of storm trajectory time series (that is, a Lagrangian view) as they evolve on an attractor.

Forecasts from a numerical weather prediction model. Given that the predictability limits appear to be short, especially for cyclone tracks, for the Weddell Sea region, it was decided that it would be a worthwhile exercise to compare the performance of a numerical weather prediction model with one of the analogue pairs. The analogue pair chosen was the second best pair, 18 July 1985 and 6 August 1986. This pair was chosen because forecasts from the operational hemisphere NWP model of the Australian Bureau of Meteorology (Bourke et al. 1977) have been archived for that period. In Fig. 6 a comparison is shown of the 500 hPa height difference from the analysis for

Fig. 6 **Analogue, persistence, and NWP forecast errors for the 500 hPa geopotential heights starting at 6 August 1986, 0000 UTC at 12-hourly intervals.**

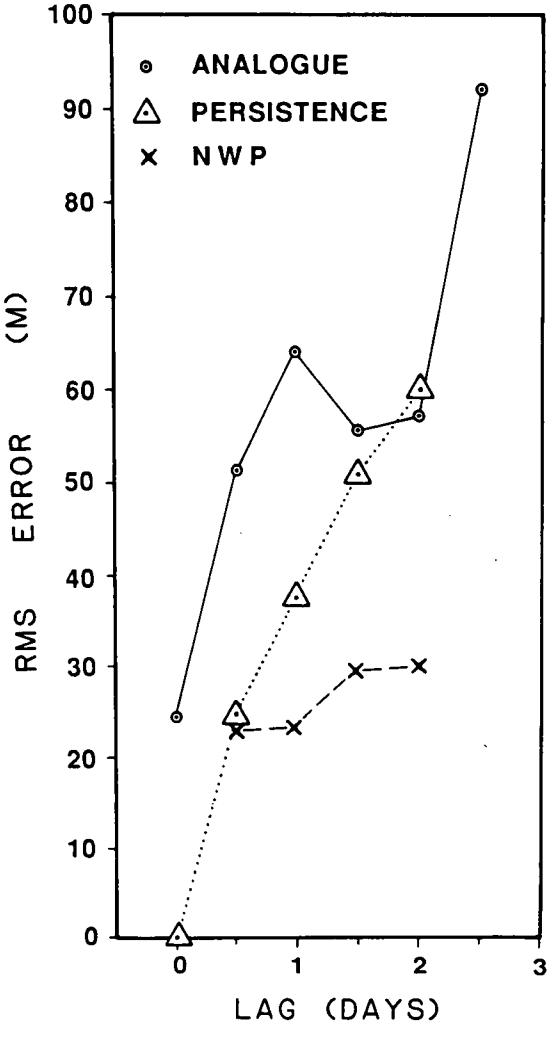

the analogue pairs and the NWP model forecast, at 12-hourly intervals out to 48 hours. For reference purposes, persistence is included.

It is immediately clear from Fig. 6 that the NWP model has a much greater level of accuracy than the analogue approach and is more accurate than persistence after 12 hours. After two days the rms error of the model is only 30 m, compared with about 60 m for the analogue and persistence. It is worth noting that the analogue of the chosen situation in this case does poorly in that the rms rises quickly to the saturation value after only 1 day whereas (from Fig. 3), on the average, it reaches saturation at about 2.5 days.

The fact that the NWP model shows skill, with rms errors of only 30 m at 2 days, is most likely due to the relatively low number of degrees of freedom observed for the high latitude synoptic-scale dynamics (Fig. 5). It appears that the NWP model can simulate the observed dynamics on the relatively low-dimensional attractor involved. It is emphasised that only one forecast has been made as the aim of the study was not to examine the predictability characteristics of the NWP model. In addition, the model predicted a number of systems, unlike the Grassberger-Procaccia theory which looked only at high latitude cyclones. Further work, which is beyond the scope of this article, will be carried out in the future on the topological structure of the model attractor to confirm that the results obtained here hold in general.

Discussion and conclusions

The main results may be summarised as follows. An attempt has been made to estimate the predictability of a sector of the Antarctic atmosphere and, in particular, the predictability of high latitude cyclone tracks. Two different types of methods were used to achieve this aim. First, an analogue method was applied to the entire sector. However, the analogues derived using the 15-year daily winter 500 hPa height fields proved to be mediocre and even the ten best analogues had a very rapid rms error doubling time of about one day. When the definition of the analogues was altered to include consecutive pairs of days, the growth rates of rms errors still remained very rapid. Second, it was decided to try an alternative, Lagrangian, method. In this technique, the algorithm of Grassberger and Procaccia (1984) was applied to 500 hPa cyclone centres. Once again a rapid rms error doubling time of about one day was found.

The results obtained from the Grassberger and Procaccia theory reveal that there is a relatively low number of degrees of freedom (about six) involved in Antarctic cyclone weather dynamics. Therefore, it is reasonable to expect that numerical weather prediction models would be able to provide skilful forecasts in high latitudes because they have many more than six degrees of freedom. This was confirmed in the single NWP case study where the NWP model forecasts were found to be the most accurate of the three techniques. It was also confirmed that analogue prediction methods have less skill than persistence. The skill of NWP model forecasts depends on the static and dynamic properties of both the processes involved and the forecast model, plus the model's ability to capture these properties from the initial data and physically simulate them.

The estimated dimension of 5–6 merely provides a lower bound of the expected degrees of

freedom governing the atmospheric dynamics; the possibility that saturation has not been reached and more degrees of freedom could be involved cannot be excluded. The amount of data is limited (500 hPa storm tracks of finite life time) and parts of the dynamics are hidden by noise. Accordingly, predictions by analogues must suffer from this deficiency so that they are able to recover only these 5–6 degrees of freedom for the prediction, whereas NWP models can resolve more details from the initial analysis and adjust them to a system of more degrees of freedom. In particular, whereas the analogues have been deduced from the 500 hPa level only, the NWP makes use of more levels; boundary conditions, which analogues disregard, can also play a crucial role. It is not, therefore, surprising that the NWP model forecasts are superior to analogue forecasts, particularly in areas where the natural growth of small errors is large. Even persistence without initial error may, in some situations, also perform better than good analogues (Fig. 2).

The estimates of predictability time-scales obtained in this study appear to be shorter than those obtained by Gutzler and Shukla (1984) who reported rms doubling times of up to a week for some limited area 500 hPa height fields. However, the present estimates are much closer to those found by Lorenz (1969) and Errico and Baumhefner (1987). In particular, Errico and Baumhefner suggested that error doubling times of the order of one day are found within active baroclinic regions. Parts of the Weddell Sea area appear to be such a region with rapidly developing and fast moving cyclones present in many of the analyses.

In conclusion, it is suggested that the predictability time-scales for cyclone tracks in the Weddell Sea area of the Antarctic are quite short, being of the order of one day in the rms error doubling sense and that the best approach in terms of practical methods for achieving these predictability limits rests with the NWP models either alone, or in combination with other statistically based methods.

Acknowledgments

Thanks are due to Mark Bass for programming assistance, Wong Hei Meng, Peter Yew and David King for technical help, and Diann Vale for typing this paper.

References

Bourke, W., McAvaney, B.J., Puri, K.K., Thurling, R. 1977. Global modeling of atmospheric flow by spectral methods. From *Methods in Computational Physics, 17, General Circulation Models of the Atmosphere*, J. Change (ed.), Academic Press, 267–324.

Eckmann, J.P. and Ruelle, D. 1985. Ergodic theory of chaos on strange attractors. *Rev. Modern Phys., 57*, 617–56.

Errico, R. and Baumhefner, D. 1987. Predictability experiments using a high-resolution limited-area model. *Mon. Weath. Rev., 115*, 488–504.

Essex, E., Lookman, T. and Nerenberg, M.A.H. 1987. The climate attractor over short time scales. *Nature, 326*, 64–6.

Fraedrich, K. 1986. Estimating the dimensions of weather and climate attractors. *J. Atmos. Sci., 43*, 331–44.

Fraedrich, K. 1987. Estimating weather and climate predictability on attractors. *J. Atmos. Sci., 44*, 722–8.

Fraedrich, K. and Leslie, L.M. 1989. Estimates of cyclone track predictability, Part I: Tropical cyclones in the Australian region. *Q. Jl R. met. Soc., 115*, 79–94.

Grassberger, P. and Procaccia, I. 1983. Estimation of the Kolmogoroff entropy from a chaotic signal. *Phys. Rev., 28A*, 2591–3.

Grassberger, P. and Procaccia, I. 1984. Dimensions and entropies of strange attractors from a fluctuating dynamics approach. *Physics, 13D*, 34–54.

Gutzler, D.S. and Shukla, J. 1984. Analogs in the wintertime 500 mb height field. *J. Atmos. Sci., 41*, 177–89.

Henderson, H.W. and Wells, R. 1988. Obtaining attractor dimensions from meteorological time series. *Adv. Geophys., 30*, 205–37.

Kalnay, E. and Livezey, R. 1985. Weather predictability beyond a week. From *Turbulence and Predictability in Geophysical Fluid Dynamics and Climate Dynamics*, M. Ghil, R. Benzi and G. Parisi (eds), North-Holland, 311–46.

Kep, S.L. 1984. A Climatology of Cyclogenesis, Cyclone Tracks and Cyclolysis in the Southern Hemisphere for the Period 1972–1981. *Publication No. 25*, Department of Meteorology University of Melbourne, 162pp.

Lorenz, E.N. 1965. A study of the predictability of a 28-variable atmospheric model. *Tellus, 27*, 321–33.

Lorenz, E.N. 1969. Atmospheric predictability. From *Problems and Prospects in Long and Medium Range Weather Forecasting*. D.M. Burridge and E. Kaellen (eds), Springer-Verlag, 1–20.

Lorenz, E.N. 1985. The growth of errors in prediction. From *Turbulence and Predictability in Geophysical Fluid Dynamics and Climate Dynamics*. M. Ghil, R. Benzi and G. Parisi (eds), North-Holland, 243–65.

Miyakoda, K., Hembree, G.D., Strickler, R.F. and Shulman, I. 1972. Cumulative results of extended forecast experiments. I. Model performance for winter cases. *Mon. Weath. Rev., 100*, 826–55.

Murphy, J.M. 1990. Assessment of the practical utility of extended range ensemble forecasts. *Q. Jl R. met. Soc., 116*, 89–125.

Packard, N.H., Crutchfield, J.D., Farmer, J.D. and Shaw, R.S. 1980. Geometry from a time series. *Phys. Rev. Lett., 45*, 712–16.

Schuster, J.G. 1988. *Deterministic Chaos*. VCH Verlag, Weinheim, 270 pp.

Shaw, D.B., Lonnberg, P., Hollingsworth, A. and Under, P. 1987. Data assimilation: The 1984/85 revisions of the ECMWF mass and wind analysis. *Q. Jl R. met. Soc., 113*, 533–66.

Smagorinsky, J. 1969. Problems and promises of deterministic extended range forecasting. *Bull. Am. met. Soc., 50*, 286–311.

Takens, F. 1981. Detecting strange attractors in turbulence. From *Dynamical Systems and Turbulence*. Warwick University, Springer-Verlag, 366–81.

Thompson, P.D. 1957. Uncertainty of initial state as a factor in the predictability of large scale atmospheric flow patterns. *Tellus, 9*, 275–95.

Tsonis, A.A. and Elsner, J.B. 1988. The weather attractor over very short time scales. *Nature, 333*, 545–7.